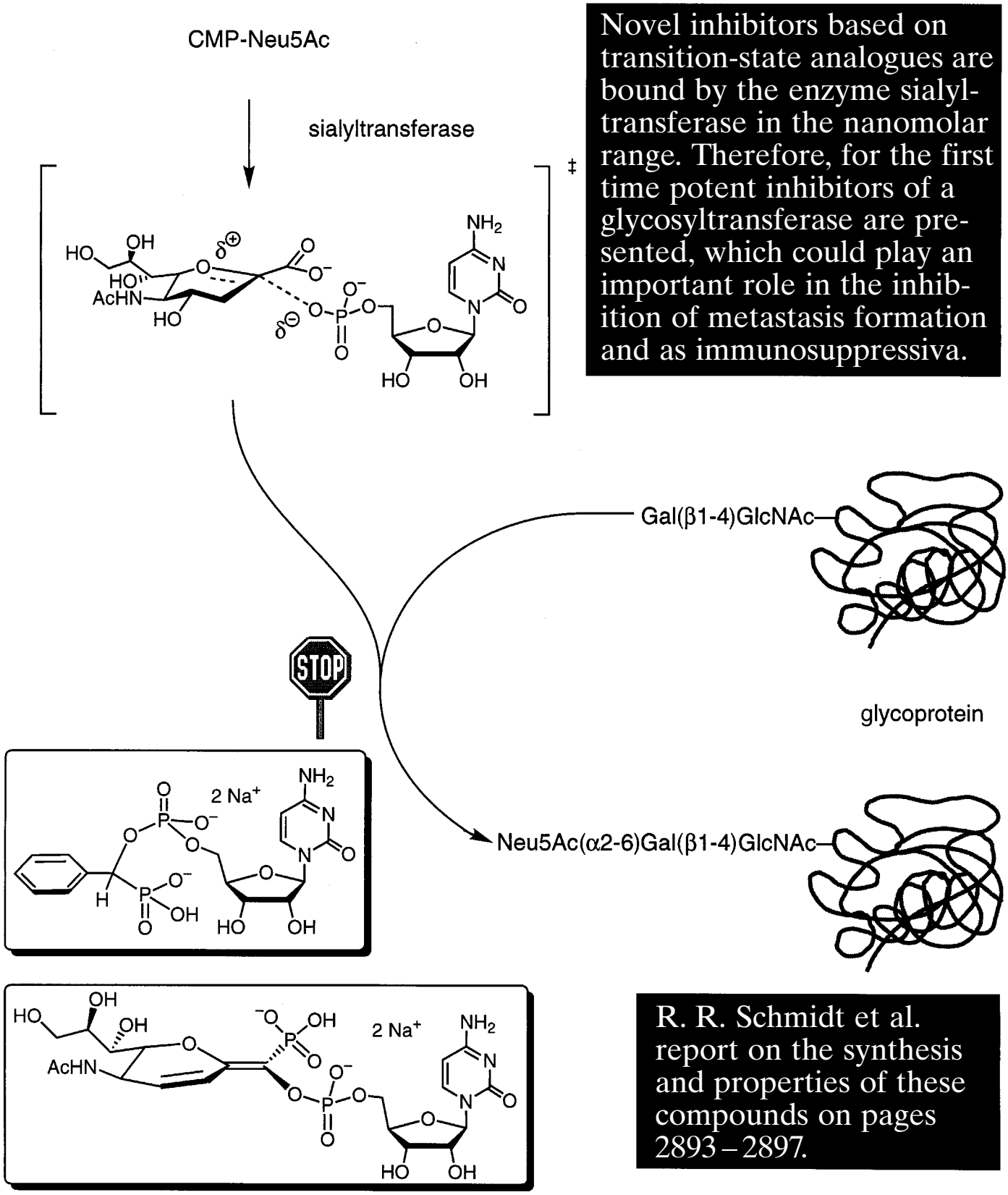

Novel inhibitors based on transition-state analogues are bound by the enzyme sialyltransferase in the nanomolar range. Therefore, for the first time potent inhibitors of a glycosyltransferase are presented, which could play an important role in the inhibition of metastasis formation and as immunosuppressiva.

R. R. Schmidt et al. report on the synthesis and properties of these compounds on pages 2893 – 2897.

Determination of End-to-End Distances in a Series of TEMPO Diradicals of up to 2.8 nm Length with a New Four-Pulse Double Electron Electron Resonance Experiment**

Rainer E. Martin, Matthias Pannier, François Diederich,* Volker Gramlich, Michael Hubrich, and Hans W. Spiess*

Organic di- and polyradicals with two or more weakly interacting unpaired electrons have received considerable attention in recent years as a result of their promising materials properties for use as organic molecular ferromagnets or superconductors.[1] Sterically shielded nitroxide radicals often exhibit a chemical inertness quite uncharacteristic of other free radicals, thus making them the subject of intense theoretical and experimental investigations. The use of such free radicals as reporter groups has rapidly evolved into one of the most powerful and versatile tools in biophysics for the study of biological systems.[2–4] In particular, the determination of distances between functional groups and the resulting topologies in biological systems[5] and amorphous solids, or the size and shape of ionic multiplets in ionomers,[6–8] is of fundamental interest and continues to attract attention as a challenging yet rewarding field of research. Unfortunately, the lack of periodic structures often severely restricts or simply prohibits the application of classical scattering techniques in such systems.

Free radicals can, however, be studied conveniently by electron paramagnetic resonance (EPR) spectroscopy.[9] This technique allows for the determination of interatomic distances of dipolar coupled electrons of up to several nanometers by making use of the dipolar coupling between the spin probes. The coupling leads to shorter longitudinal relaxation times (T_1) and phase memory times (T_m), which have been used for estimating distances in spin-labeled iron porphyrins.[10] Quantitative determination of distances, however, requires more sophisticated techniques, such as pulsed double electron electron resonance (DEER) spectroscopy, which was pioneered by Milov and Tsvetkov[11] and Larsen and Singel.[12]

To the best of our knowledge, this technique has so far not been applied for the quantitative determination of unknown structures. Only first attempts to study end-to-end distances in a series of aliphatic hydrocarbons have been reported.[13] This situation is partly a consequence of technical limitations of pulsed EPR (dead time),[14] but also because of the lack of such measurements for a series of compounds with well-defined end-to-end distances ranging up to several nanometers. Here we provide such a data set by extending the three-pulse DEER sequence[13] to a four-pulse sequence that generates an echo and therefore, overcomes the dead-time problem. The systems studied are the TEMPO diradicals **1a**–**e** (R = Si*t*BuMe$_2$) in which the two TEMPO moieties are linked by rigid, conjugated spacers with large, well-defined end-to-end distances. Such compounds are of particular interest as precursors (models) for highly conjugated polymers for electronic, photonic, and optical applications.[15]

4,4′-(Butadiyne-1,4-diyl)bis(4-hydroxy-2,2,6,6-tetramethylpiperidine-*N*-oxyl) (BIPO, **1a**)[16] was synthesized by a new, simple, and short route (Scheme 1a). The slow addition of a solution of lithiated triisopropylsilylacetylene in THF by syringe pump to a solution of 2,2,6,6-tetramethyl-4-oxopiperidine-*N*-oxyl (**2**)[17] in THF at 0 °C gave **3** in 64% yield. Interestingly, the X-ray crystal structure analysis of **3** disclosed that the triisopropylsilylacetylene residue, rather than the hydroxyl group, adopts the axial position (Figure 1).[18] The analysis of the crystal lattice showed that intermolecular hydrogen bonding is not at the origin of the observed conformational preference, since the nitroxyl oxygen atom and the hydrogen atom of the hydroxyl group of neighboring molecules are at a distance of 4.57 Å. Subsequent removal of the silyl protecting group of **3** with *n*Bu$_4$NF in wet THF afforded the free acetylene derivative **4** (96% yield), which was oxidatively dimerized under Hay conditions[19] to give **1a**[16a] in 79% yield. In the synthesis of diradicals **1b**–**e** (Scheme 1B), addition of dilithiated (*E*)-3,4-bis[(*tert*-butyldimethylsilyloxy)methyl]hex-3-ene-1,5-diyne (**5**)[20] or *p*-diethynylbenzene (**6**)[21] to a solution of **2** (2 equiv) in THF in the presence of high concentrations of LiBr (up to 10 equiv)[22] afforded both mono- and bis-coupled products (**7**: 28%, **1b**:

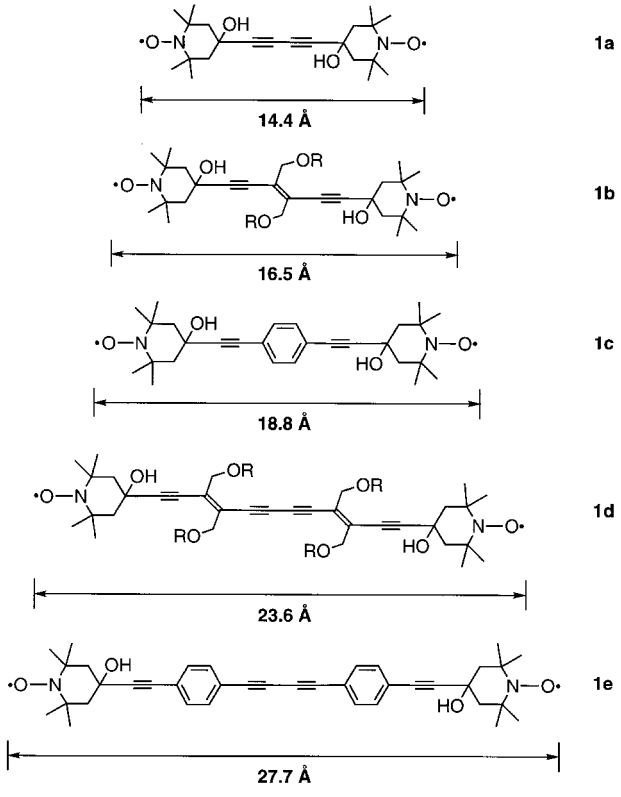

[*] Prof. Dr. F. Diederich, Dipl.-Chem. R. E. Martin
Laboratorium für Organische Chemie, ETH Zentrum
Universitätstrasse 16, CH-8092 Zurich (Switzerland)
Fax: (+41) 1-632-1109
E-mail: diederich@org.chem.ethz.ch
Prof. Dr. H. W. Spiess, Dipl.-Phys. M. Pannier, Dr. M. Hubrich
Max-Planck-Institut für Polymerforschung
Postfach 3148, D-55021 Mainz (Germany)
Fax: (+49) 6131-379-100
E-mail: spiess@mpip-mainz.mpg.de
[**] Prof. Dr. V. Gramlich
Laboratorium für Kristallographie, ETH Zentrum
Sonneggstrasse 5, CH-8092 Zürich (Switzerland)

  1433-7851/98/3720-2834 $ 17.50+.50/0

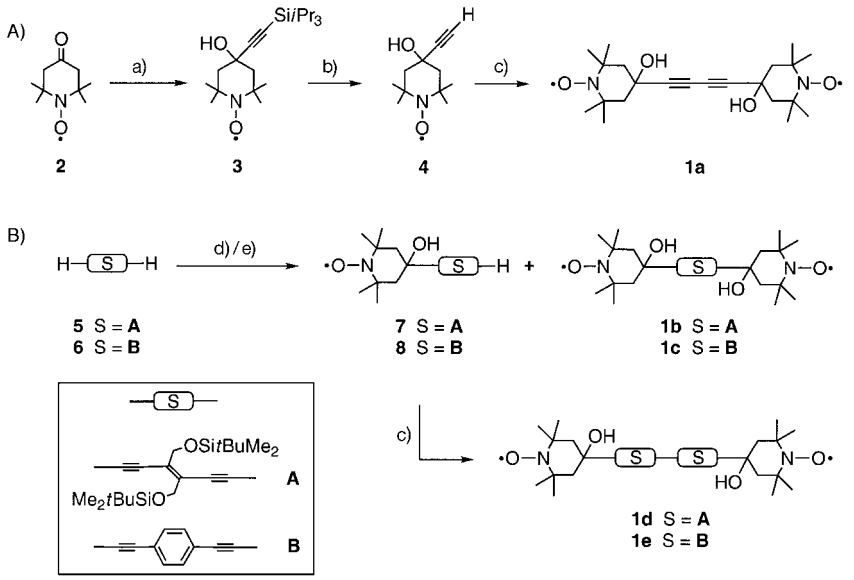

Scheme 1. Preparation of TEMPO diradicals **1a**–**e**. Reagents and conditions: a) iPr$_3$C≡CH, nBuLi, THF, 0 °C, 1 h, then 20 °C, 2 h, 64 %; b) nBu$_4$NF, wet THF, 96 %; c) CuCl, *N*,*N*,*N*′,*N*′-tetramethylethylenediamine (TMEDA), O_2, CH_2Cl_2, 4-Å molecular sieves, 3 h, **1a**: 79 %, **1d**: 55 %, **1e**: 86 %; d) **5**, nBuLi (2 equiv), anhydrous LiBr (10 equiv), **2**, THF, 0 °C, 1 h then 20 °C, 2 h, **7**: 28 %, **1b**: 39 %; e) **6**, nBuLi (2 equiv), anhydrous LiBr (1 equiv), **2**, THF, 0 °C, 1 h, then 20 °C, 2 h, **8**: 25 %, **1c**: 9 %.

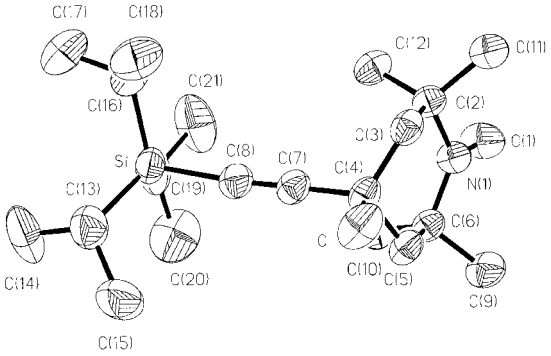

Figure 1. Molecular structure of TEMPO radical **3**. The ORTEP drawing depicts thermal ellipsoids at the 30 % probability level. Selected bond lengths [Å] and angles [°]: O(1)–N(1) 1.283(4), N(1)–C(2) 1.494(5), C(2)–C(3) 1.520(6), C(3)–C(4) 1.516(6), C(4)–C(7) 1.465(7), C(7)–C(8) 1.208(6); O(1)-N(1)-C(2) 115.5(3), N(1)-C(2)-C(3) 109.6(3), C(2)-C(3)-C(4) 117.9(3), C(3)-C(4)-C(7) 113.9(3), C(4)-C(7)-C(8) 176.5(4).

39 %, and **8**: 25 %, **1c**: 9 %). Oxidative Hay coupling of **7** and **8** led to the diradicals **1d** and **1e**, respectively (Table 1).

The analysis of the DEER signals closely follows that of the conventional three-pulse DEER experiment, as described by the groups of Tsvetkov[11] and Singel.[12] The time-domain signal I_{4p}(DEER) consists of two exponentials that lie back to back and are superimposed by a modulation [Eqs. (1)–(4)],

$$I_{4p}(\mathrm{DEER})(\Delta t) = \cos(\omega_{AB}\Delta t)\exp(kCF_B\Delta t) \quad (1)$$

$$\omega_{AB} = \omega_{DD}(3\cos^2\theta_{AB} - 1) \quad (2)$$

$$k = \frac{8\pi^2\mu_B^2 g_A g_B}{9\hbar\sqrt{3}} \qquad \omega_{DD} = \frac{\mu_B^2 g_A g_B}{\hbar}\frac{1}{r_{AB}^3} \quad (3, 4)$$

where C is the concentration of the unpaired electron spins, F_B the fraction of electron spins excited by the microwave pulse at frequency ν_2 (Figure 2), μ_B the Bohr magneton, g_A and g_B the g factors of the respective electron, and r_{AB} the electron–electron distance. Furthermore, $\Delta t = t_B - 2\tau$ (Figure 2), θ_{AB} is the angle between the magnetic field B_0 and the dipolar axis that connects the two electrons, and ω_{DD} is the dipolar coupling constant in angular frequency units. Equation (1) describes an oscillation with frequency $\nu_{AB} = \omega_{AB}/2\pi$ which arises from the superimposition of the dipolar coupling between the two unpaired electrons within the diradical on an exponential decay, and reflects the much weaker dipole–dipole coupling between different diradicals.[23, 24]

The information about the end-to-end distance r_{AB} is encoded in ω_{AB}. For a powder an average value over the different orientations of end-to-end vectors has to be taken, which results in a spectrum with two singularities that correspond to $\theta_{AB} = 90°$, resembling the well-known Pake spectrum of a spin pair in nuclear magnetic resonance.[25]

The symmetric four-pulse DEER time-domain signal of the longest diradical (**1e**)

Table 1. Selected physical data of **1b**-**e**.[a]

1b: M.p. 124–125 °C; UV/Vis (EtOH): λ_{max} (ε) = 270 (25400), 277 nm (22600, sh); FT-IR ($CHCl_3$): $\tilde{\nu}$ = 3689m, 3589m, 3300m, 3000m, 2958s, 2933s, 2856s, 2356m, 2332m, 1600m, 1494w, 1472m, 1463m, 1433w, 1421w, 1379w, 1361m, 1343m (N-O•), 1261m, 1237w, 1183m, 1100s, 1006m, 939w, 915w, 891w, 839s cm^{-1}; FAB-MS: m/z: 707.5 (100, [MH$_3^+$]), 706.4 (90, [MH$_2^+$]), 705.4 (37, [MH$^+$]), 704.4 (33, [M^+]), 692.4 (16, [MH$_3$ – CH$_3$]$^+$), 691.4 (36, [MH$_2$ – CH$_3$]$^+$), 690.4 (53, [MH – CH$_3$]$^+$), 689.4 (84, [M – CH$_3$]$^+$); elemental analysis calcd for $C_{38}H_{68}N_2O_6Si_2$ (705.15): C 64.73, H 9.72, N 3.97; found: C 64.73, H 9.50, N 3.74.

1c: M.p. 182–183 °C; UV/Vis (EtOH): λ_{max} (ε) = 212 (18400), 217 (18100), 270 (42100), 282 nm (41700); FT-IR ($CHCl_3$): $\tilde{\nu}$ = 3622s, 3467m, 3011s, 2978s, 2889m, 2467w, 1600w, 1483w, 1444w, 1396w, 1373w, 1342w (N–O•), 1250w, 1044s, 878m cm^{-1}; FAB-MS: m/z: 469.3 (100, [MH$_3$]$^+$), 468.3 (28, [MH$_2$]$^+$), 467.3 (10, [MH]$^+$), 466.3 (5, [M]$^+$); HR-FAB-MS: m/z: found: 469.3077 ([MH$_3$]$^+$, $^{12}C_{28}H_{41}N_2O_4^+$); calcd: 469.3066; elemental analysis calcd for $C_{28}H_{38}N_2O_4 \cdot 0.5\,H_2O$ (475.63): C 70.71, H 8.26, N 5.89; found: C 70.30, H 8.04, N 5.70.

1d: M.p. 114 °C (decomp); UV/Vis (EtOH): λ_{max} (ε) = 267 (26600), 280 (27200), 294 (25600), 314 (21600), 343 (25800), 367 nm (22700); FT-IR ($CHCl_3$): $\tilde{\nu}$ = 3689w, 3589m, 3360w, 3000m, 2959s, 2933s, 2856s, 2356m, 2332m, 1600m, 1472m, 1463m, 1379w, 1361m, 1343w (N–O•), 1256m, 1237w, 1100s, 1042w, 1020w, 1006w, 939w, 916w, 891w, 839s cm^{-1}; FAB-MS: m/z: 1053.4 (16, [MH$_3$ – O]$^+$), 1052.4 (31, [MH$_2$ – O]$^+$), 1051.4 (38, [MH – O]$^+$), 1050.4 (29, [M – O]$^+$), 632.2 (100); HR-FAB-MS: m/z: found: 1051.6842 ([MH – O]$^+$, $^{12}C_{58}H_{103}N_2O_7{}^{28}Si_4$), calcd: 1051.6842.

1e: m.p. 169–170 °C (decomp); UV/Vis (EtOH): λ_{max} (ε) = 224 (17100), 233 (15100), 261 (17000), 277 (18400), 292 (24600), 310 (33400), 332 (41000), 356 nm (35000); FT-IR ($CHCl_3$): $\tilde{\nu}$ = 3622s, 3467m, 3022s, 2974s, 2889m, 1444w, 1389w, 1342w (N–O•), 1250m, 1044s, 878m cm^{-1}; EI-MS: m/z: 593.2 (3, [MH$_3$]$^+$), 592.2 (6, [MH$_2$]$^+$), 591.1 (10, [MH]$^+$), 590.2 (3, [M]$^+$), 559.2 (92, [M – HNO]$^+$), 140.0 (100); HR-EI-MS: m/z: found: 590.3136 (M^+, $^{12}C_{38}H_{42}N_2O_4^+$), calcd: 590.3144.

[a] All new compounds described were fully characterized by melting point, FT-IR and UV/VIS spectroscopy, EI or FAB mass spectrometry, and high-resolution mass spectrometry and/or correct elemental analysis.

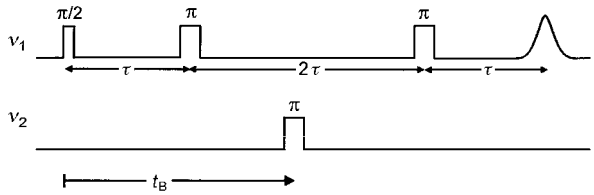

Figure 2. The newly developed four-pulse DEER sequence consists of a refocused echo at microwave frequency ν_1 and a π pulse at ν_2, which is incremented in time. The time t_B is the incrementation time which starts at $t_B = \tau$ and ends at $t_B = 3\tau$. τ is the fixed evolution time of the refocused Hahn echo pulse sequence. All microwave pulses utilized were of a duration of 32 ns and had a frequency difference of $\Delta\nu = 60$ MHz.

of the series recorded at 15 K in a polystyrene matrix is shown in Figure 3a. The exponentials and the superimposed modulation are clearly visible. After subtraction of the exponential decay and Fourier transformation a Pake-type spectrum is obtained (Figure 3b). In contrast to the conventional DEER experiment where only singularities can be observed, broad contributions to the line shape are observable with the four-pulse DEER sequence.[12, 13] This substantial advantage and improvement is a consequence of the absence of dead time in the four-pulse DEER experiment and allows for the first time to measure broad distributions of dipolar couplings.

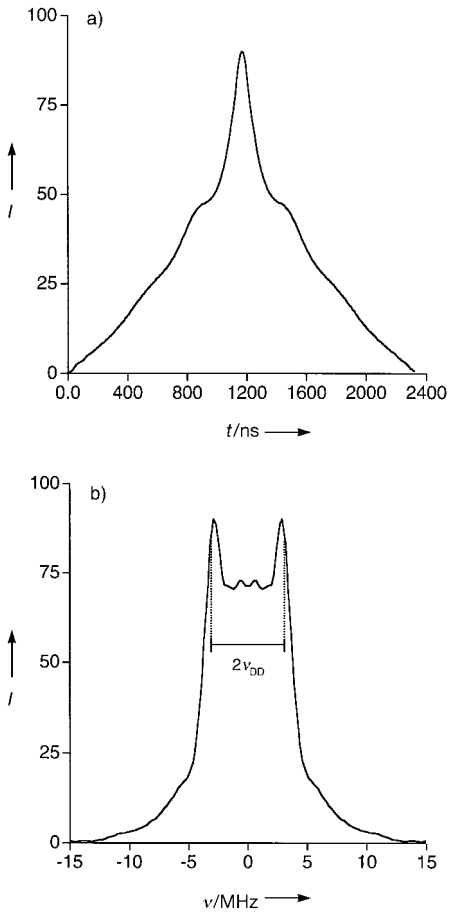

Figure 3. a) Four-pulse DEER time-domain signal of diradical **1e** mixed into polystyrene at 15 K. All pulses had a length of $t_P = 32$ ns and the evolution time τ had a duration of 1200 ns. b) Four-pulse DEER spectrum of **1e** as obtained by Fourier transformation of the time-domain data in a) after subtracting two exponentials and zero filling. The bar indicates the distance $2\nu_{DD}$ between the two singularities of an unbroadened Pake pattern that fits the experimental spectrum.

In the present study, the singularities that define the dipolar coupling constant and thus the electron–electron distance are very narrow and clearly recognizable. Only the "foot" of the Pake spectrum is not visible, as would be expected from orientation selection owing to only partial excitation of the inhomogenously broadened EPR spectrum of ^{14}N-labeled nitroxide.[12] The measured coupling constants and calculated electron–electron distances for the series **1a–e** are given in Table 2, together with results of molecular dynamics simulations, which revealed averaged end-to-end distances from 1.5 nm (**1a**) to 2.8 nm (**1e**).[26]

Table 2. Dipolar coupling constants ν_{DD} and interradical distances r_{AB} obtained for **1a–e** by molecular dynamics simulations and experimentally measured data.

Compd	ν_{DD} [MHz]	$\Delta\nu_{DD}$[a] [MHz]	r_{AB}^{th}[b] [Å]	r_{AB}^{exp}[c] [Å]
1a	–	–	14.4 ± 1.0	–
1b	14.16	0.49	16.5 ± 1.0	15.4 ± 0.2
1c	10.25	0.49	18.8 ± 1.0	17.2 ± 0.3
1d	4.88	0.49	23.6 ± 1.0	22.0 ± 0.7
1e	3.05	0.49	27.7 ± 1.0	25.7 ± 1.4

[a] Experimental error of the dipolar coupling constant. [b] Averaged distances estimated from molecular dynamics simulations, measured from oxygen to oxygen of the terminal N–OH groups.[26] [c] Experimentally obtained distances.

The uncertainty of about ± 1 Å is not from spectroscopic limitations, but reflects the conformational freedom of the nitroxide spin labels, which result from the axial/equatorial positions of the alkyne substituents on the six-membered rings as well as from rotations about the C(sp)–C(sp^3) bonds. For the shortest diradical **1a**, no experimental coupling constant could be obtained, since it was not possible to apply microwave π pulses shorter than 32 ns, as would be necessary to excite the dipolar subspectra. This bandwidth problem leads to a lower interradical distance limit for the present method of approximately 1.5 nm. On the other hand, at least five full oscillations with the frequency corresponding to the singularities in the Pake pattern should be observable in an interval of length τ for a precise distance determination (see Figure 3b). The length of the whole sequence (4τ) should not exceed the phase memory time T_m considerably for sensitivity reasons. Both requirements combined let us expect an upper distance limit of about 8 nm for the method to be applicable. Experimental and estimated distances are in good agreement, considering the fact that the DEER experiments were performed in a matrix at 15 K, while molecular dynamics simulations were done in the gas phase at ambient temperature. The experimental distances appear to be systematically shorter than the calculated ones by about 8%, but we refrain from drawing any conclusions from that.

With the diradical series **1a–e**, we have demonstrated the amenability of advanced Fourier transformation electron electron double resonance spectroscopy for measuring electron–electron distances in the range of 1.6 to 2.8 nm. This provides a base for applying this technique to more complex

  1433-7851/98/3720-2836 $ 17.50+.50/0

systems, where intergroup distances might not be so well defined. We are currently exploring the practical limits of the four-pulse DEER experiment for the determination of distance distributions up to the theoretical limit which is expected to be about 8 nm.

Experimental Section

Typical procedure for the coupling of lithiated acetylenes and TEMPO radical **2**. Compounds **1b** and **7**: A solution of *n*BuLi (0.17 mL, 0.28 mmol, 1.6 M solution in *n*-hexane) was added slowly to a solution of **5** (0.050 g, 0.138 mmol) and anhydrous LiBr (0.12 g, 1.38 mmol) in dry THF (30 mL) under N_2 at 0 °C, and the mixture was stirred for 30 min. Subsequently, a solution of **2** (0.12 g, 0.69 mmol) in dry THF (4 mL, over 4-Å molecular sieves) was introduced by syringe pump within 1 h, and the solution stirred for an additional 2 h at 20 °C. The mixture was diluted with a saturated solution of aquous NH_4Cl (100 mL) and extracted with CH_2Cl_2, and the organic phase was dried ($MgSO_4$). Separation by flash chromatography (SiO_2, *n*-hexane/AcOEt 5/1) furnished **7** (0.021 g, 28 %) as a slightly orange solid, and purification of the residue by preparative thin layer chromatography (SiO_2, *n*-hexane/AcOEt 1/1) yielded **1b** (0.038 g, 39 %) as an orange solid.

Typical procedure for oxidative Hay couplings. Compound **1d**: TMEDA (0.016 mL, 0.11 mmol) and CuCl (0.003 g, 0.03 mmol) were added over 5 min to a solution of **7** (0.042 g, 0.079 mmol) in dry CH_2Cl_2 (5 mL) over 4-Å molecular sieves at 20 °C. After the mixture had been stirred in air for 3 h, a solution of EDTA (EDTA = ethylenediaminetetraacetic acid, pH 8) was added, and the mixture extracted with CH_2Cl_2 until the washings remained colorless. The organic phase was washed with a saturated aqueous solution of NaCl and dried ($MgSO_4$). Purification by flash chromatography (SiO_2, *n*-hexane/AcOEt 3/1) afforded **1d** (0.023 g, 55 %) as an orange solid.

Distance determination. The four-pulse DEER measurements were performed on a modified Bruker ESP380E X-band Fourier transformation spectrometer. One channel of the microwave pulse-forming unit was used for a second microwave frequency. An HP-86290B RF plug-in module in an HP-8350B sweep oscillator was employed as the source for the second frequency. The output microwave of the HP-86290B RF plug-in module was increased by an amplifier from Miteq (AMF-5S-8012-18). The probehead used was a commercial electron nuclear double resonance (ENDOR) resonator from Bruker (EN4118X-MD4), which was overcoupled for obtaining a broad resonator resonance line. The resolution of four-pulse DEER experiments depends on the length of the constant time interval 2τ. For the precise determination of long distances we used $\tau =$ 1200 ns. This in turn necessitated a measurement temperature of 15 K to ensure that enough signal was left despite phase relaxation for a period of 4.8 μs. The choice of a difference of 60 MHz between the two microwave frequencies enabled us to work with a single-mode resonator yet still excite transitions of the two nitroxide moieties selectively.

Received: April 21, 1998 [Z11762IE]
German version: *Angew. Chem.* **1998**, *110*, 2994 – 2998

Keywords: diradicals · double electron electron resonance spectroscopy · EPR spectroscopy

[1] a) A. Rajca, *Chem. Rev.* **1994**, *94*, 871 – 893; b) J. S. Miller, A. J. Epstein, *Angew. Chem.* **1994**, *106*, 399 – 432; *Angew. Chem. Int. Ed. Engl.* **1994**, *33*, 385 – 415; c) J. S. Miller, *Adv. Mater.* **1992**, *4*, 435 – 438; d) J. H. Zhang, A. J. Epstein, J. S. Miller, C. J. O'Connor, *Mol. Cryst. Liq. Cryst.* **1989**, *176*, 271 – 276; e) D. W. Wiley, J. C. Calabrese, J. S. Miller, *Mol. Cryst. Liq. Cryst.* **1989**, *176*, 277 – 288.

[2] J. F. W. Keana, *Chem. Rev.* **1978**, *78*, 37 – 64.

[3] *Spin Labeling-Theory and Applications* (Ed.: L. J. Berliner), Academic Press, London, **1976**.

[4] "Resolved Electron-Electron Spin-Spin Splittings in EPR Spectra": G. R. Eaton, S. S. Eaton in *Biological Magnetic Resonance*, *Vol. 8* (Eds.: L. J. Berliner, J. Reuben), Plenum, New York, **1989**, pp. 339 – 398.

[5] Y.-K. Shin, C. Levinthal, F. Levinthal, W. L. Hubbel, *Science* **1993**, *259*, 960 – 963.

[6] *Ionomers*, *Characterization*, *Theory*, *and Applications* (Ed.: S. Schlick), CRC, New York, **1996**.

[7] V. Schädler, A. Franck, U. Wiesner, H. W. Spiess, *Macromolecules* **1997**, *30*, 3832 – 3838.

[8] V. Schädler, V. Kniese, T. Thurn-Albrecht, U. Wiesner, H. W. Spiess, *Macromolecules* **1998**, submitted.

[9] J. E. Wertz, J. R. Bolton, *Electron Spin Resonance*, McGraw-Hill, New York, **1972**.

[10] M. H. Rakowsky, K. M. More, A. V. Kulikov, G. R. Eaton, S. S. Eaton, *J. Am. Chem. Soc.* **1995**, *117*, 2049 – 2057.

[11] a) A. D. Milov, K. M. Salikhov, M. D. Shirov, *Fiz. Tverd. Tela* **1981**, *23*, 975 – 982; b) A. D. Milov, A. B. Ponomarev, Y. D. Tsvetkov, *Chem. Phys. Lett.* **1984**, *110*, 67 – 72.

[12] R. G. Larsen, D. J. Singel, *J. Chem. Phys.* **1993**, *98*, 5134 – 5146.

[13] V. Pfannebecker, H. Klos, M. Hubrich, T. Volkmer, A. Heuer, U. Wiesner, H. W. Spiess, *J. Phys. Chem.* **1996**, *100*, 13428 – 13432.

[14] *Modern Pulsed and Continuous-Wave Electron Spin Resonance* (Eds.: L. Kevan, M. K. Bowman), Wiley, New York, **1990**.

[15] *Electronic Materials: The Oligomer Approach* (Eds.: K. Müllen, G. Wegner), Wiley-VCH, Weinheim, **1997**.

[16] a) P. G. Hamill, A. E. Yost, J. D. Sandman, *Mol. Cryst. Liq. Cryst. Sci. Technol. Sect. A* **1992**, *211*, 339 – 346; b) J. S. Miller, D. T. Glatzhofer, J. C. Calabrese, A. J. Epstein, *J. Chem. Soc. Chem. Commun.* **1988**, 322 – 323; c) Yu. V. Korshak, T. V. Medvedeva, A. A. Ovchinnikov, V. N. Spector, *Nature (London)* **1987**, *326*, 370 – 372.

[17] a) M. B. Neiman, E. G. Rozantzev, Yu. G. Mamedova, *Nature (London)* **1962**, *196*, 472 – 474; b) G. Sosnovsky, M. Konieczny, *Synthesis* **1976**, 735 – 736; c) for a review on the chemistry of hindered piperidines, see M. Dagonneau, E. S. Kagan, V. I. Mikhailov, E. G. Rozantsev, V. D. Sholle, *Synthesis* **1984**, 895 – 916.

[18] X-ray crystal structure of **3** at 293 K: $C_{20}H_{38}NO_2Si$, $M_r = 352.6$, triclinic space group $P\bar{1}$, $\rho_{calcd} = 1.056$ g cm^3, $Z = 4$, $a = 7.741(9)$, $b = 8.516(10)$, $c = 33.80(3)$ Å, $\alpha = 91.84(8)$, $\beta = 92.46(8)$, $\gamma = 94.41(9)^\circ$, $V = 2218(4)$ Å^3. Data were measured on an Syntex P21 diffractometer with $Mo_{K\alpha}$ radiation ($\lambda = 0.71073$ Å) with ω scans. The structure was solved by direct methods and refined by full-matrix least-squares analysis (SHELXTL PLUS; heavy atoms anisotropic, H atoms fixed, whereby H positions are based on stereochemical considerations) to give $R1 = 0.0663$, $wR2 = 0.1711$ for 4142 independent observed reflections and 570 variables [$I \geq 2.0\sigma(I)$, $2.4 \leq \theta \leq 20.0^\circ$]. Crystallographic data (excluding structure factors) for the structure reported in this paper have been deposited with the Cambridge Crystallographic Data Centre as supplementary publication no. CCDC-101294. Copies of the data can be obtained free of charge on application to CCDC, 12 Union Road, Cambridge CB2 1EZ, UK (fax: (+44) 1223-336-033; e-mail: deposit@ccdc.cam.ac.uk).

[19] A. S. Hay, *J. Org. Chem.* **1962**, *27*, 3320 – 3321.

[20] R. R. Tykwinski, M. Schreiber, R. Pérez Carlón, F. Diederich, V. Gramlich, *Helv. Chim. Acta* **1996**, *79*, 2249 – 2281.

[21] S. Takahashi, Y. Kuroyama, K. Sonogashira, N. Hagihara, *Synthesis* **1980**, 627 – 630.

[22] P. E. van Rijn, S. Mommers, R. G. Visser, H. D. Verkruijsse, L. Brandsma, *Synthesis* **1981**, *116*, 459 – 460.

[23] K. M. Salikhov, S. A. Dzuba, A. M. Raitsimring, *J. Magn. Reson.* **1981**, *42*, 255 – 276.

[24] V. V. Kurshev, A. M. Raitsimring, Y. D. Tsvetkov, *J. Magn. Reson.* **1989**, *81*, 441 – 454.

[25] A. Abragam, *The Principles of Nuclear Magnetism*, Clarendon, Oxford, **1983**.

[26] CVFF force field, Insight II (Version 95.0), Biosym Technologies, San Diego, **1995**. Instead of N–O$^\bullet$, the parameter set for the N – OH group was used for the simulations. Hartman et al. recommended the use of a C=O group as a surrogate for the nitroxyl N – O$^\bullet$ moiety in performing simulations (D. Hartmann, R. Philipp, K. Schmadel, J. J. Birktoft, L. J. Banaszak, W. E. Trommer, *Biochemistry* **1991**, *30*, 2782 – 2790). However, the error introduced in the end-to-end distance measurements by using N–OH instead of C=O and performing the simulations in the absence of solvent molecules is more than outweighted by the conformational freedom of the nitroxide spin labels arising from the axial/equatorial positions of the alkyne substituents on the six-membered rings and the rotations about the C(sp) – C(sp^3) bonds.

  1433-7851/98/3720-2837 $ 17.50+.50/0